Inorganic Chemistry

Article

pubs.acs.org/IC

Formazanate Ligands as Structurally Versatile, Redox-Active Analogues of β-Diketiminates in Zinc Chemistry

Mu-Chieh Chang,[†] Peter Roewen,[†] Raquel Travieso-Puente,[†] Martin Lutz,[‡] and Edwin Otten*[,†]

[†]Stratingh Institute for Chemistry, University of Groningen, Nijenborgh 4, 9747 AG Groningen, The Netherlands

[‡]Bijvoet Center for Biomolecular Research, Crystal and Structural Chemistry, Utrecht University, Padualaan 8, 3584 CH Utrecht, The Netherlands

Supporting Information

ABSTRACT: A range of tetrahedral bis(formazanate)zinc complexes with different steric and electronic properties of the formazanate ligands were synthesized. The solid-state structures for several of these were determined by X-ray crystallography, which showed that complexes with symmetrical, unhindered ligands prefer coordination to the zinc center via the terminal N atoms of the NNCNN ligand backbone. Steric or electronic modifications can override this preference and give rise to solid-state structures in which the formazanate ligand forms a 5-membered chelate by binding to the metal center via an internal N atom. In solution, these compounds show dynamic equilibria that involve both 5- and 6-membered chelates. All compounds are intensely colored, and the effect of the ligand substitution pattern on the UV−vis absorption spectra was evaluated. In addition, their cyclic voltammetry is reported, which shows that all compounds may be electrochemically reduced to radical anionic (L_2Zn^-) and dianionic (L_2Zn^{2-}) forms. While unhindered NAr substituents lie in the plane of the ligand backbone (Ar = Ph), the introduction of sterically demanding substituents (Ar = Mes) favors a perpendicular orientation in which the NMes group is no longer in conjugation with the backbone, resulting in hypsochromic shifts in the absorption spectra. The redox potentials in the series of L_2Zn compounds may be altered in a straightforward manner over a relatively wide range (~700 mV) via the introduction of electron-donating or -withdrawing substituents on the formazanate framework.

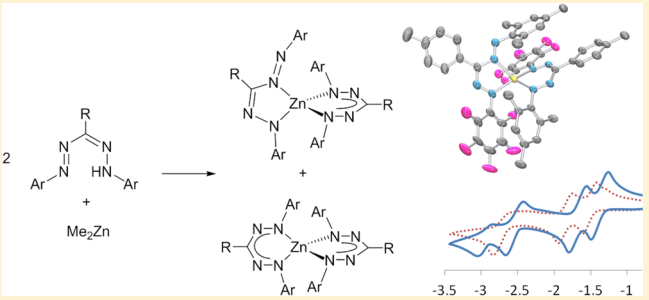

INTRODUCTION

Ligands that contain conjugated 5-membered π systems have been a cornerstone for the development of organometallic chemistry. Cyclopentadienyl anions and their derivatives provide a unique steric/electronic environment that allows the synthesis and characterization of a vast array of main-group and transition-metal complexes. More recently, metal complexes with noncyclic (hetero)pentadienyls have been investigated.[1] The 1,5-diazapentadienyls [β-diketiminate or nacnac; nitrogen analogues of acetylacetonate (acac)] allow facile tuning through substitution at the N atoms. These ligands have become increasingly popular and are now a benchmark ligand in organometallic chemistry and catalysis, with metal complexes known across the periodic table.[2] Complexes of related monoanionic 1,3,5-triazapentadienyls were initially reported by Siedle et al.[3] and Dias et al.,[4] while zinc and magnesium complexes with 1,3,5-triazapentadienyl ligands were reported by Anders et al.[5] and Zhou et al.,[6] respectively. The coordination chemistry of neutral 1,3,5-triazapentadienes was also studied by the groups of Würthwein[7] and Pombeiro.[8] The analogous 1,2,4,5-tetraaza compounds are better known as "formazans", and their organic chemistry has been studied quite extensively.[9] Interest in these compounds originates from their intense color, which may be exploited in dyestuffs,[10] in trace metal analysis (Zincon),[11] or as redox-based staining agents in cell biology (histochemistry).[12]

Despite the structural similarities between β-diketiminate (**A**), 1,3,5-triazapentadienyl (**B**), and formazanate (**C**) in Chart 1, the coordination chemistry of formazanate ligands has remained relatively little explored. Hicks and co-workers reported some well-characterized examples of late-transition-metal formazanate complexes,[13] and boron compounds with formazanate ligands were shown to possess unusual redox properties.[14] We have recently communicated our initial results on bis(formazanate)zinc compounds, in which we demonstrated these complexes to be stable in three oxidation states,

Chart 1. Monoanionic Azapentadienyl Ligands

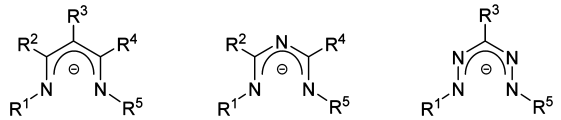

Received: October 28, 2014
Published: December 10, 2014

   dx.doi.org/10.1021/ic5025873 | Inorg. Chem. 2015, 54, 379−388

with the formazanate ligands functioning as electron reservoirs.[15] Furthermore, novel boron derivatives with these ligands were recently reported by us[16] and the group of Gilroy,[17] in which it was shown that formazanates may exist in three different redox states ($L^{1-/2-/3-}$). In the present contribution, we describe a series of bis(formazanate)zinc complexes to delineate the effects of steric and electronic modifications in the formazanate ligand on the structure of the resulting complexes. In addition, we show how these changes modulate the electronic spectra and redox properties of these compounds.

RESULTS AND DISCUSSION

Ligand Synthesis. A general route to the formazan framework is provided by the two-step route depicted in Scheme 1. Condensation of an aldehyde with aromatic

Scheme 1. General Synthetic Procedure for the Preparation of Formazans

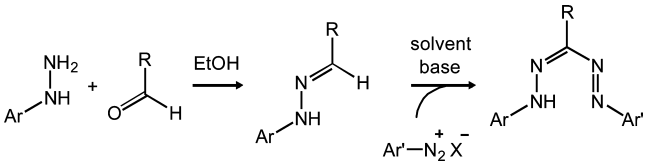

hydrazines affords the desired hydrazone derivatives, which are treated in a subsequent step with a diazonium salt in the presence of a base to produce intensely colored reaction mixtures from which the desired formazan can be isolated in moderate yields.[9] The modular nature of this synthetic procedure allows the introduction of a variety of different substitution patterns, including asymmetric derivatives. As a starting point, we synthesized the known formazan PhNNC(*p*-tolyl)NNHPh (L1H) in a biphasic reaction medium via the procedure published by Hicks and co-workers.[14] The coupling of trimethylacetaldehyde–phenylhydrazone with phenyldiazonium chloride afforded the bis(phenyldiazenyl)methane compound PhNNCH(^{t}Bu)NNPh (L2H), which does not spontaneously tautomerize to the corresponding formazan.[18] Deprotonation of L2H, however, is facile and results in a delocalized formazanate anion (vide infra). Attempts to prepare the somewhat more sterically demanding asymmetric derivative MesNNC(*p*-tolyl)NNHPh (L3H) by treatment of the hydrazone (*p*-tolyl)CH=NNHPh with $MesN_2^+$ (either prepared in situ as the chloride or isolated as the BF_4 salt)[19] resulted in intensely colored reaction mixtures from which we were unable to isolate the formazan. Changing the solvent in which the reaction was conducted to acetone/water with NaOH as the base yielded the product MesNNC(*p*-tolyl)-NNHPh (L3H) in moderate yield upon crystallization from CH_2Cl_2/MeOH. The symmetrical derivative MesNNC(*p*-tolyl)NNHMes (L4H) required yet another solvent mixture: this sterically demanding formazan could be obtained in low yield (11%) from the coupling of $MesN_2Cl$ with (*p*-tolyl)CH=NNHMes in MeOH with NaOH/NaOAc.[20] Using similar synthetic procedures, electron-poor formazans with C_6F_5 substituents at either the terminal N atoms [PhNNC(*p*-tolyl)NNH(C_6F_5) (L5H) and MesNNC(*p*-tolyl)NNH(C_6F_5) (L6H)] or the backbone C atom [PhNNC(C_6F_5)NNHMes (L7H)] were obtained. Formazan derivatives with an electron-withdrawing cyano group on the central C atom can be isolated from the direct coupling of cyano acetic acid with 2 equiv of aryldiazonium salts under basic conditions.[9] Using this strategy, we prepared the formazan MesNNC(CN)NNHMes (L8H). In related nacnac chemistry, 2,6-disubstituted aromatic rings have become popular because they provide steric protection above and below the coordination plane; we anticipate that the mesityl groups in our formazanate ligands will behave similarly.

Synthesis of Bis(formazanate)zinc Complexes. The treatment of Me_2Zn with 2 equiv of formazan L1H results in complete conversion of the starting materials. The ^{1}H NMR spectrum of the product is consistent with its formulation as the homoleptic bis(formazanate) complex $[L1]_2Zn$ (**1**), with diagnostic resonances for the *p*-tolyl and phenyl moieties in a 1:2 ratio. Compound **1** was isolated in 76% yield as dark-violet crystals upon crystallization from toluene/hexane. The ligands L2H–L4H reacted similarly, and good yields of the corresponding bis(formazanate)zinc complexes (**2**–**4**) were isolated as intensely colored crystalline materials (Scheme 2).[15]

Scheme 2. Synthesis of Bis(formazanate)zinc Compounds 1–4

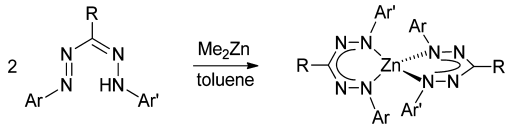

L1H	Ar = Ar' = Ph; R = *p*-tolyl	$[L1]_2Zn$ (**1**)
L2H	Ar = Ar' = Ph; R = ^{t}Bu	$[L2]_2Zn$ (**2**)
L3H	Ar = Ph; Ar' = Mes; R = *p*-tolyl	$[L3]_2Zn$ (**3**)
L4H	Ar = Ar' = Mes; R = *p*-tolyl	$[L4]_2Zn$ (**4**)

Single-crystal X-ray diffraction studies on compounds **1**–**4** showed in all cases a central Zn atom surrounded by two formazanate ligands in a tetrahedral coordination environment (Figure 1; pertinent bond distances and angles are given in Table 1). The formazanate bite angles differ little for the unhindered, symmetric derivatives **1** and **2** [Ar = Ar′; N–Zn–N 90.38(5)–93.18(7)°], while in the cases of **3** and **4**, the N–Zn–N angles are somewhat smaller, with values between 87.98(4)° and 88.76(7)°. The dihedral angle between the planes that contain the two N–Zn–N fragments deviates from the ideal tetrahedral value of 90°, with values between 83.64(11)° and 86.43(7)° for the symmetrical derivatives and only 71.26(6)° for asymmetric complex **3**. Full delocalization within the formazanates in **1**–**4** is indicated by the equivalent N–N and C–N bond lengths in the backbone of each ligand. Upon increasing steric hindrance of the NAr substituents, the NNCNN backbone becomes increasingly puckered and the Zn atom is displaced out of the ligand plane, similar to what is observed in related *β*-diketiminatezinc [(nacnac)Zn] complexes, where an envelope conformation of the (nacnac)Zn 6-membered ring is observed.[21] The NPh rings in **1**–**3** are found to be approximately coplanar with the ligand backbone (NNCNN/Ph dihedral angles < 20°), a situation that maximizes conjugation. However, steric interactions in **3** and **4** between the 2,6-Me_2 groups on the NMes substituents and the ligand backbone cause these groups to have much larger dihedral angles (75.65° in **3** and 64.74–80.14° in **4**). In the solid-state structure of complex **3**, the NMes rings are oriented nearly parallel (interplanar angle = 3.21° and distance between centroids = 3.660 Å) and stack in an off-center fashion, as is usually observed for electron-rich aromatic rings.[22]

dx.doi.org/10.1021/ic5025873 | *Inorg. Chem.* 2015, 54, 379–388

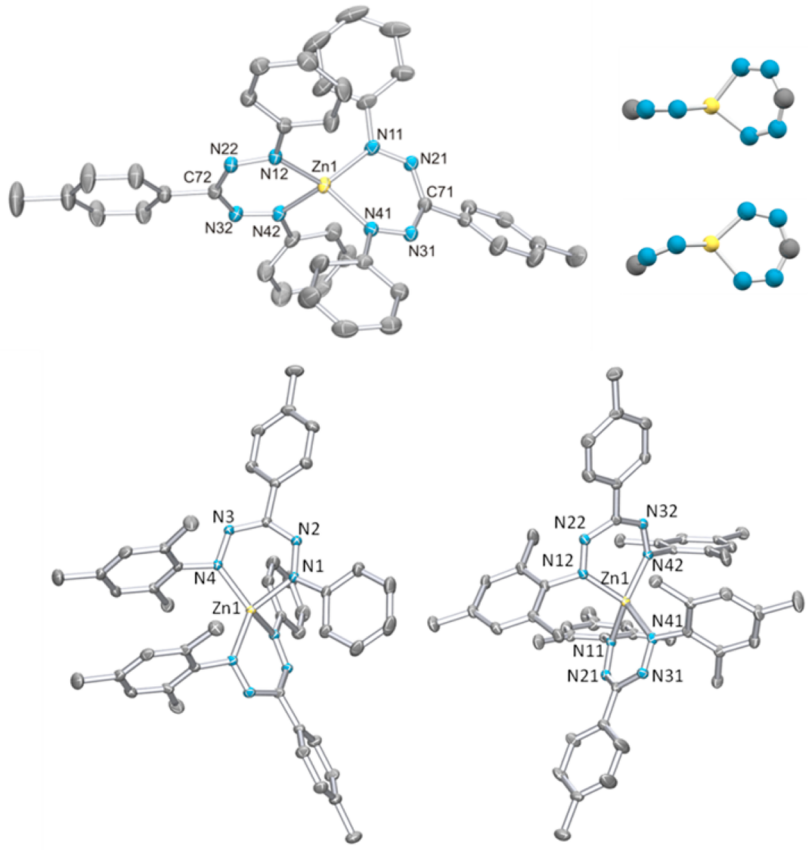

Figure 1. Top: Molecular structure of **1** showing 50% probability ellipsoids (left). View along both NNCNN planes in **1** (right). Bottom: Molecular structures of **3** (left) and **4** (right) showing 50% probability ellipsoids (all H atoms and solvent molecules omitted for clarity).

Table 1. Selected Bond Distances and Angles for Compounds 1−4

	1		**2**[c]		**3**	**4**	
	x = 1	x = 2	x = 1	x = 2	x = none	x = 1	x = 2
Zn1−N1x	1.9849(11)	1.9829(12)	1.9824(17)	1.9902(17)	2.0179(10)	1.9874(16)	2.0234(16)
Zn1−N4x	1.9953(12)	2.0012(12)	1.9822(18)	1.9769(18)	1.9882(10)	2.0207(16)	1.9873(16)
N1x−N2x	1.3067(16)	1.3120(16)	1.310(2)	1.307(2)	1.3026(14)	1.310(2)	1.303(2)
N3x−N4x	1.3048(16)	1.3024(16)	1.307(2)	1.309(2)	1.3129(14)	1.304(2)	1.310(2)
N2x−$C_{backbone}$[a]	1.3462(18)	1.3464(18)	1.340(3)	1.353(3)	1.3504(15)	1.343(2)	1.357(3)
N3x−$C_{backbone}$[a]	1.3517(18)	1.3499(18)	1.343(3)	1.332(3)	1.3512(16)	1.353(2)	1.345(3)
N1x−Zn1−N4x	92.21(5)	90.38(5)	93.18(7)	92.94(7)	87.98(4)	88.76(7)	88.03(7)
N−Zn−N/N−Zn−N[b]	86.43(7)		83.64(11)		71.26(6)	85.07(9)	
Ar/NNCNN	14.26, 19.86	18.99, 36.30	3.32, 14.11	4.45, 18.88	18.98 (Ph), 75.65 (Mes)	76.50, 80.14	64.74, 75.21

[a] $C_{backbone}$ is the central C atom of the ligand backbone. [b] The angle between the planes defined by the central Zn atom and the coordinated N atoms. [c] One of two independent molecules is discussed.

The NMR spectroscopic features for the symmetrical complexes **1**, **2**, and **4** are straightforward and consistent with equivalent NAr groups in both ^{1}H and ^{13}C NMR spectra. The room temperature ^{1}H NMR spectrum of **3** shows the CH and *o*-Me groups of the mesityl rings to be equivalent, which suggests that rotation around the N−Mes bond is facile. However, the resonances due to the *o*-Me groups are somewhat broadened, and cooling a toluene-d_8 solution to −25 °C results in decoalescence of these signals to afford an NMR spectrum that is consistent with the solid-state structure of **3**.

The observed structural deformations in **3** that result from the (sterically) asymmetric formazanate ligand prompted the synthesis of analogues with two electronically disparate NAr substituents. The treatment of ArNNC(*p*-tolyl)NNH(C_6F_5) (Ar = Ph, L5H; Ar = Mes, L6H) with Me_2Zn in a 2:1 molar ratio results in the formation of the desired complexes $[L5]_2Zn$ (**5**) and $[L6]_2Zn$ (**6**) (Scheme 3). We were unable to crystallize compound **5**, so that purification was difficult. Nevertheless, the reaction is clean, and careful control of the reaction stoichiometry gave **5** in >95% purity, as assessed by ^{1}H NMR spectroscopy. The analogous mesityl-substituted compound **6** was isolated in 71% yield as a dark-violet crystalline material.

A single-crystal X-ray structure determination showed compound **6** to be an unusual bis(formazanate)zinc complex in which two distinct ligand-binding modes are observed (Figure 2; pertinent bond distances and angles are given in

dx.doi.org/10.1021/ic5025873 | *Inorg. Chem.* 2015, 54, 379−388

Scheme 3. Synthesis of Compounds 5 and 6

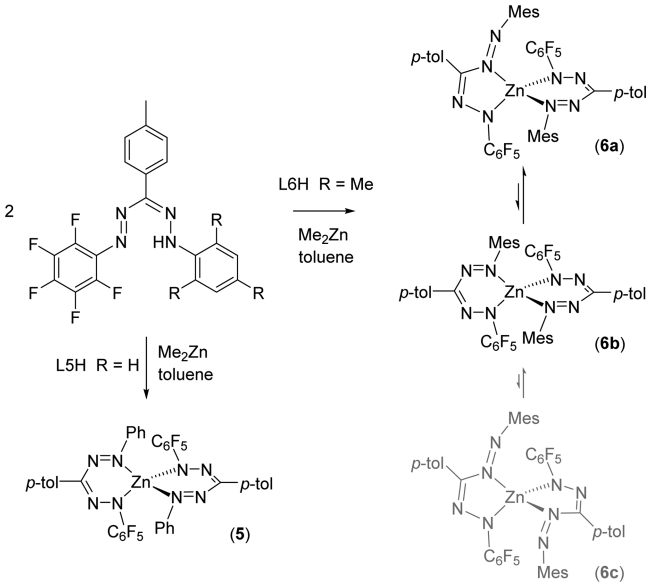

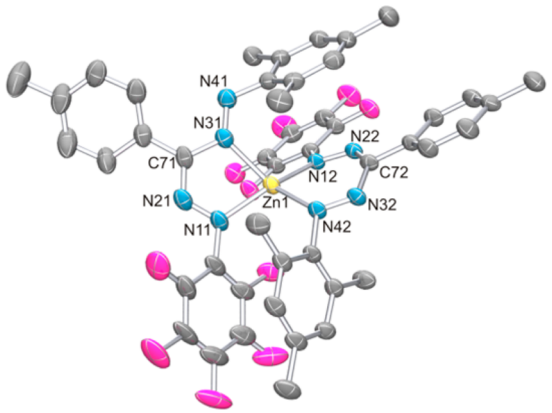

Figure 2. Molecular structure of **6** showing 50% probability ellipsoids. The H atoms are omitted for clarity.

Table 2). One of the formazanates is bound in the "normal" fashion to generate a 6-membered chelate ring, whereas the other ligand is coordinated through both the terminal N11 and an internal N31 atom, resulting in a 5-membered chelate. As expected, the ligand bite angles differ considerably at 78.93(9)° and 88.90(9)° for the 5 and 6-membered rings, respectively. Balt and co-workers described the formation of an intermediate en route to copper and nickel complexes with the formazan (2-OHPh)NNC(Ph)NNHPh, which they tentatively identified as isomers with a 5-membered formazanate chelate ring,[23] and a crystal structure was reported for the nickel derivative.[24] Furthermore, large structural diversity in alkali-metal formazanate complexes was recently reported by us that includes 4- and 5-membered chelate rings.[25] The structural relationship observed between the ubiquitous β-diketiminates and the formazanate ligands for compounds **1**–**4** no longer holds in complex **6**: the presence of the additional N atoms in the backbone that can function as donor atoms favors the formation of a 5-membered chelate ring that is not accessible for β-diketiminates.[2] The energetic balance, however, is quite subtle because 5- and 6-membered rings are observed simultaneously in **6**. A closer inspection of the N–N and N–C bond lengths within the formazanate frameworks (Table 2) shows that both ligands are best described with a localized negative charge at the C_6F_5-substituted N atom: the observed bond length alternation contrasts the delocalization in **1**–**4**; the more localized nature is likely the result of the strong electron-withdrawing effect of the C_6F_5 ring. Whereas **3** shows off-center stacking of two mesityl rings, in compound **6**, there is a face-centered interaction of an electron-poor C_6F_5 ring with an electron-rich mesityl group (interplanar angle = 5.31°; centroid–centroid distance = 3.375 Å), indicative of an aromatic donor–acceptor interaction that is commonly observed for combinations of electron-rich/poor rings.[22]

Characterization of the structures of **5** and **6** by solution NMR spectroscopy reveals remarkable differences. Compound **5** shows one set of resonances for the NPh and N(C_6F_5) groups, consistent with a coordination geometry around the Zn center similar to that found in **1**–**4**. For **6**, a larger number of resonances than expected was observed in the ^{1}H NMR, independent of the batch of material and despite the fact that the isolated crystals seemed homogeneous. Invariably, three distinct sets of formazanate resonances were observed in both the ^{1}H and ^{19}F NMR spectra at room temperature in an approximate 1:0.7:0.7 ratio. Careful consideration of the ^{1}H and ^{19}F NMR data allows us to assign these to two different isomeric compounds (**6a** and **6b**, in a 1.4:1 ratio) that differ in the coordination environment around the Zn center. For the major species (**6a**), the formazanate ligands are inequivalent, in agreement with the 5- and 6-membered chelate rings observed

Table 2. Selected Metrical Parameters for 6, 8, and 9

	6		8		9[b]
	x = 1	x = 2	x = 1	x = 2	x = 1
Zn1–N1x	1.988(2)	1.998(2)	1.9877(13)	1.9550(14)	2.135(4)
Zn1–N3x	2.094(2)		2.0890(15)		2.175(3)
Zn1–N4x		2.001(2)		1.9711(14)	
N1x–N2x	1.322(4)	1.321(3)	1.310(2)	1.3035(19)	1.281(5)
N3x–N4x	1.284(3)	1.287(3)	1.277(2)	1.3042(19)	1.327(5)
N2x–$C_{backbone}$[a]	1.323(4)	1.324(3)	1.338(2)	1.345(2)	1.395(6)
N3x–$C_{backbone}$[a]	1.395(4)	1.379(3)	1.378(2)	1.351(2)	1.306(6)
N1x–Zn1–N3x	78.92(10)		79.85(5)		74.23(13)
N1x–Zn1–N4x		88.90(9)		92.63(6)	
N–Zn–N/N–Zn–N	59.44(14)		78.43(8)		

[a] $C_{backbone}$ is the central C atom of the ligand backbone. [b] One of the two independent molecules is discussed.

dx.doi.org/10.1021/ic5025873 | Inorg. Chem. 2015, 54, 379–388

Scheme 4. Synthesis of Compounds 7 and 8

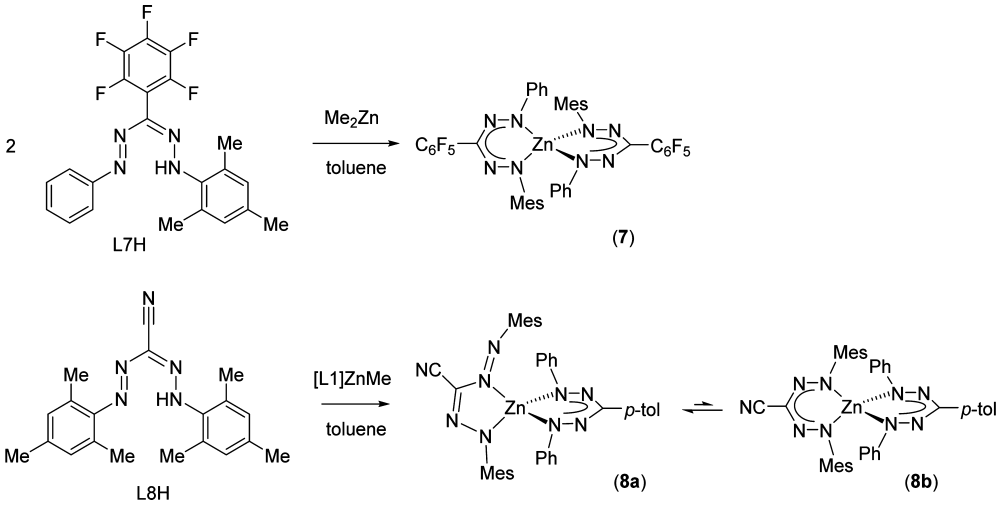

in the solid-state structure of **6**. The minor species (**6b**) shows equivalent formazanate ligands, on the basis of which we assign this to possess two 6-membered chelate rings (Scheme 3). The equilibrium constant between these two species was determined by a variable-temperature NMR study, which resulted in $\Delta H = -3.3$ kJ·mol^{-1} and $\Delta S = -14$ J·mol^{-1}·K^{-1}. The decrease in the entropy on going to isomer **6b** is in agreement with a more crowded coordination sphere in the case of two 6-membered chelate rings. Moreover, the π-stacking interactions observed in the solid-state structure (**6a**) are likely lost in isomer **6b**. The negative value for ΔH indicates that a 6-membered chelate ring is enthalpically favored. In the ^{19}F NMR spectra of **6**, a third isomer (**6c**) is observed as a very minor component (<5%; see the Supporting Information, SI): a ^{19}F EXSY NMR experiment confirms its participation in the equilibrium with **6a**/**6b**. This isomer has equivalent NC_6F_5 groups, which suggests that the formazanate ligands in **6c** bind to the metal center with two 5-membered chelate rings (Scheme 3).

Synthesis of the bis(formazanate)zinc complex **7** with a C_6F_5 substituent at the central C atom of the ligand framework was previously reported by us[16] and is included here for comparison (Scheme 4). While the compound could not be crystallized, it is likely that **7** contains two 6-membered ring chelates: the steric properties of the ligand are very similar to those in **3**, and both formazanates are equivalent in the ^{1}H NMR.

Bis(formazanate)zinc complexes with two different formazanate ligands are accessible via the monoligand zinc methyl complex [L1]ZnMe, which is obtained from a 1:1 reaction of L1H with Me_2Zn.[26] Stirring [L1]ZnMe with 1 equiv of L8H results in formation of the mixed complex [L1][L8]Zn (**8**; Scheme 4). In the solid-state structure of **8** (Figure 3; bond distances and angles are given in Table 2), two different formazanate binding motifs are found that are similar to those in **6**: the formazanate ligands L1 and L8 form 6- and 5-membered chelate rings, respectively, that have quite different bite angles [92.63(6)° and 79.85(5)°]. The mesityl-substituted ligand L8 adopts a 5-membered chelate ring to minimize steric interactions. The N−N and N−C bond lengths within the 5-membered chelate ring are indicative of localized single and double bonds. The ^{1}H NMR spectrum of a crystalline sample of **8** in a C_6D_6 solution shows the presence of two isomers in approximately a 1:0.2 ratio. For the major isomer (**8a**), the

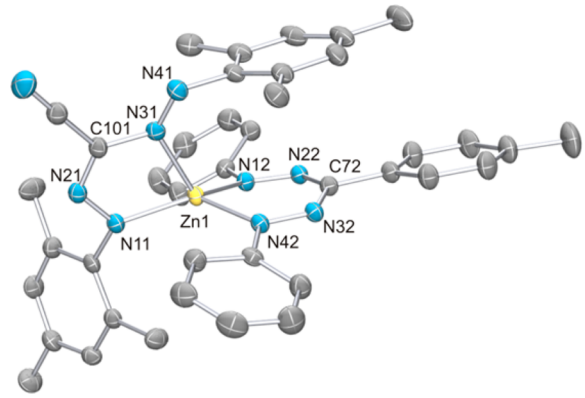

Figure 3. Molecular structure of **8** showing 50% probability ellipsoids. The H atoms are omitted for clarity.

ligand L1 appears as a symmetric set of resonances with equivalent NPh groups, while ligand L8 is asymmetrically bound, as indicated by inequivalent NMes moieties. The minor isomer (**8b**) is fully symmetric. Evidence for exchange between the isomers comes from the observation of exchange crosspeaks in the EXSY spectrum between the two species at 100 °C in a toluene-d_8 solution (no exchange is observed at room temperature). The intensities of the signals due to the minor isomer change only slightly when the temperature is increased from 0 °C (major:minor = 1:0.17) to 100 °C (1:0.29). Evaluation of the equilibrium constant at four different temperatures between 0 and 100 °C allows the enthalpy and entropy terms to be determined as $\Delta H = +4.7$ kJ·mol^{-1} and $\Delta S = +2.5$ J·mol^{-1}·K^{-1}. In contrast to complex **6**, two 6-membered formazanate chelate rings are enthalpically disfavored for **8**, while there is hardly any preference based on entropy.

Using the less basic zinc reagent $Zn(C_6F_5)_2$, deprotonation of added formazan is considerably slower than that in the case of Me_2Zn, and it was possible to isolate a complex in which the parent formazan L1H is coordinated to the metal center. After stirring of an equimolar mixture of $Zn(C_6F_5)_2$ and L1H in toluene for 15 min and subsequent crystallization from toluene/hexane at −80 °C, the compound $[L1H]Zn(C_6F_5)_2$ (**9**) could be isolated as dark-reddish crystals in 57% yield. A slightly broadened resonance at 8.20 ppm in the ^{1}H NMR spectrum indicates the presence of a NH moiety. An X-ray

dx.doi.org/10.1021/ic5025873 | Inorg. Chem. 2015, 54, 379−388

crystal structure determination confirmed this proposal. The crystal undergoes a solid−solid phase transition during cooling (see the Experimental Section), and we will only discuss the ordered structure at 100(2) K (Figure 4; bond distances and

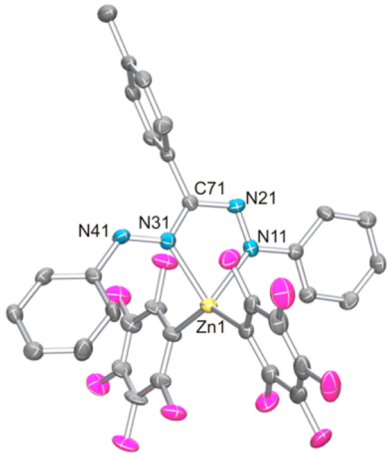

Figure 4. Molecular structure of **9** showing 50% probability ellipsoids. The H atoms and toluene solvent molecules are omitted for clarity. Only one of two independent molecules is shown.

angles are given in Table 2). The central Zn atom is surrounded by two C_6F_5 groups and two N atoms from the formazan. The Zn−C_6F_5 bond distances [2.000(4) and 1.986(4) Å] are in the range normally observed in compounds of the type L_2Zn-$(C_6F_5)_2$.[27] The formazan ligand is bonded through a terminal and internal N atom with distances of 2.135(4) and 2.175(3) Å, respectively. As expected, the Zn−N distances are longer than those observed in the compounds containing anionic formazanate ligands. The variation in the N−N and N−C bond lengths within the formazan backbone is similar to that observed in the 5-membered chelate rings in formazanate compounds **6** and **8**.

UV−Vis Spectroscopy. The optical properties of the bis(formazanate)zinc complexes were measured by UV−vis absorption spectroscopy in a THF solution. All compounds show intense absorption bands with extinction coefficients between 17000 and 50000 $L{\cdot}mol^{-1}{\cdot}cm^{-1}$ in the visible range of the spectrum (between 450 and 600 nm), which are due to $\pi-\pi^*$ transitions within the formazanate framework (Figure 5). The symmetrical derivatives absorb most strongly, and introducing an electron-donating ^{t}Bu group instead of a *p*-tolyl moiety results in a blue shift in the absorption maximum

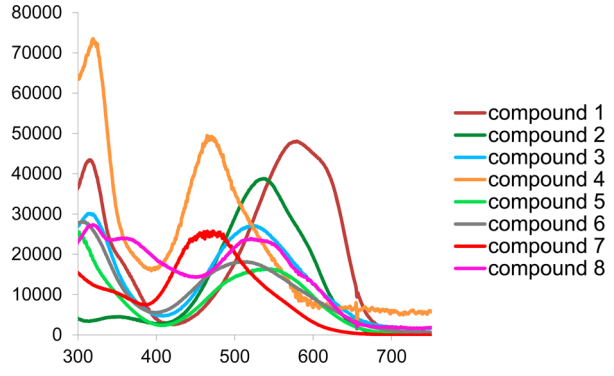

Figure 5. Absorption spectra for compounds **1**−**8** in THF.

(578 and 536 nm for **1** and **2**, respectively). Upon substitution of NPh for NMes groups, λ_{max} is progressively blue-shifted from 578 (**1**) to 520 (**2**) to 465 nm (**3**). This likely results from the perpendicular orientation of the NMes rings, which prevents conjugation between the formazanate backbone and the NAr substituent, thereby limiting the length of the π-conjugated system.[17] A similar trend is observed for compounds **5** and **6**, but this comparison is complicated by the presence of an isomer mixture for **6**. Complex **7**, with a C_6F_6 substituent on the central C atom of the ligand, has the lowest absorption wavelength of the series with λ_{max} = 463 nm.

Cyclic Voltammetry (CV). In a previous communication, we showed that the formazanate ligands in **1** and **2** can be stepwise and reversibly reduced to the corresponding radical anions (L_2Zn^-) and diradical dianions (L_2Zn^{2-}).[15] With a significantly enlarged series of bis(formazanate)zinc complexes in hand, a study of their electrochemical properties was conducted. In all cases, quasi-reversible redox processes were observed, with two independent, sequential reductions taking place to transform L_2Zn to L_2Zn^- and subsequently to L_2Zn^{2-} (Figure S1 in the SI). The data presented here are recorded in THF with a $[Bu_4N][PF_6]$ electrolyte, whereas $[Bu_4N][B(C_5F_5)_4]$ was used in our previously reported work: the data for compounds **1** and **2** with $[Bu_4N][PF_6]$ are included here to facilitate comparison (Table 3). For all compounds, the

Table 3. Electrochemical Parameters for Bis(formazanate) zinc Complexes[a]

			E^0 vs $Fc^{0/+}$ [V]		
	N−Ar[b]	C−R[c]	$L_2Zn^{0/1-}$ (I/I′)	$L_2Zn^{1-/2-}$ (II/II′)	Δ [V]
1	Ph_2	*p*-tol	−1.39	−1.68	0.29
2	Ph_2	^{t}Bu	−1.52	−1.84	0.32
3	Ph/Mes	*p*-tol	−1.60	−1.99	0.39
4	Mes_2	*p*-tol	−1.86	−2.30	0.44
5	Ph/C_6F_5	*p*-tol	−1.17	−1.57	0.40
6	Mes/C_6F_5	*p*-tol	−1.34	−1.82	0.48
7	Ph/Mes	C_6F_5	−1.41	−1.87	0.46
7[d]	Ph/Mes	C_6F_5	−1.41	−1.81	0.40
8	Mes_2 Ph_2	CN *p*-tol	−1.33	−1.82	0.49

[a]1.5 mM solution of a zinc complex in THF; 0.1 M $[Bu_4N][PF_6]$ electrolyte, scan rate = 100 $mV{\cdot}s^{-1}$. [b]Aromatic substituents at the formazanate terminal N atoms. [c]Substituent at the formazanate backbone C atom. [d]In a dichloroethane solution.

difference between the first and second reduction potentials ranges between 0.29 V for **1** and 0.48 V for **6**. As expected, changing the electron-withdrawing *p*-tolyl substituent on the C atom of the formazanate backbone (**1**: −1.38/−1.68 V vs $Fc^{0/+}$) for an electron-donating ^{t}Bu group (**2**: −1.52/−1.84 V vs $Fc^{0/+}$) shifts the redox potentials to more negative values by ∼0.15 V. A similar effect is observed for the N substituents: a donating mesityl group shifts the reduction potential to more negative values in comparison to phenyl (for **3**: −1.60 and −1.99 V vs $Fc^{0/+}$). Two NMes groups, as in **4**, show redox chemistry that occurs at even more negative potential (−1.86 and −2.30 V vs $Fc^{0/+}$). Conversely, electron-withdrawing NAr groups shift the observed redox potentials in the positive direction, and a similar effect is observed for a CC_6F_5 group such as in **7**. Although the substituent on the central C atom of the formazanate ligand does not contribute to the redox-active molecular orbital,[15,28] inductive effects are apparently equally

dx.doi.org/10.1021/ic5025873 | Inorg. Chem. 2015, 54, 379−388

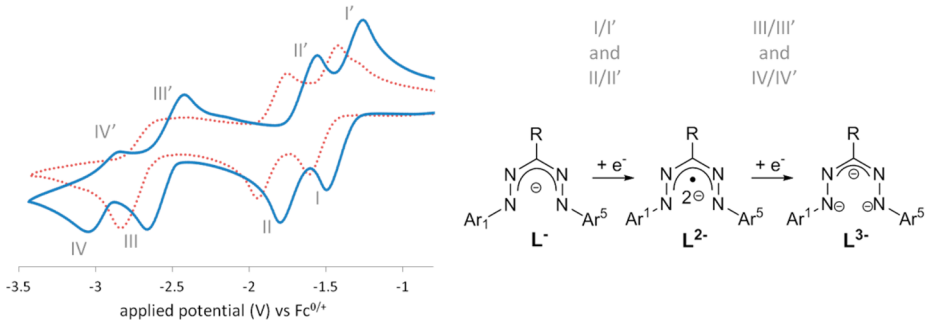

Figure 6. Cyclic voltammograms of compounds **1** (line) and **2** (dotted line) (ca. 1.5 mM solution of a zinc complex in THF; 0.1 M $[Bu_4N][PF_6]$ electrolyte; scan rate = 100 mV·s^{-1}) showing the presence of reduction waves corresponding to two-electron reduction of a single formazanate ligand (L^{3-}, reductions III and IV).

important in modulating the redox potentials of these compounds. The cyclic voltammograms indicate that, for all compounds studied here, two separate redox events occur corresponding to sequential ligand-based reductions from L_2Zn to the radical anion L_2Zn^- and the dianion L_2Zn^{2-}, all of which are quite stable based on the quasi-reversible nature of the CV peaks. For some compounds (most prominently in **4**), features in addition to that of simple reversible electron transfer were observed. We have not investigated this in detail, but we tentatively assign it to the occurrence of a subsequent chemical step that could be isomerization from 6- to 5-membered chelate ring(s).

We recently showed that, for (formazanate)BF_2 compounds, two-electron reduction of a single formazanate ligand is possible.[16] We therefore attempted the further reduction of L_2Zn compounds by scanning the CV toward more negative potentials (Figure 6). For compound **1**, two additional redox events were recorded at ca. −2.55 and −2.95 V vs $Fc^{0/+}$ to give a total of five accessible oxidation states for this compound ($L_2Zn^{0/1-/2-/3-/4-}$). For the related compound **2**, only one additional reduction wave was observed between −2.5 and −3.5 V vs $Fc^{0/+}$ (peak potential −2.84 V), corresponding to the $L_2Zn^{2-/3-}$ couple, and this reduction is much less reversible on the basis of the voltammetric response. Nevertheless, these data indicate that two-electron reduction of a single formazanate ligand to give L^{3-}-type structures could be general.

Conclusions. The synthesis of a set of sterically and electronically diverse formazans has allowed the preparation of a series of L_2Zn complexes. On the basis of detailed structural investigations, both in the solid state and in solution, it is evident that these ligands are not just isostructural, N-rich analogues of β-diketiminates. The internal N atoms in the NNCNN backbone of formazanates can function as donor atoms, thus leading to significantly enhanced flexibility in its coordination behavior. Sterically demanding NAr groups can lead to 5-membered chelate rings bound in an *N*NCN*N* fashion instead of the "normal" coordination through the terminal N atoms (*N*NCN*N*). This coordination mode is accessible reversibly, as evidenced by the observation of equilibria, and results in decreased steric pressure around the metal center. We anticipate that this feature may be useful in the application of formazanates as supporting ligands in which the coordination environment around the metal center can adapt to accommodate the binding of substrates. The CV data show reversible ligand-based redox chemistry for all compounds regardless of the substitution pattern on the formazanate ligands, which give access to the redox series $L_2Zn^{0/1-/2-}$. Moreover, in some cases, additional reductions were observed, corresponding to two-electron reduction of each formazanate ligand (accessing $L_2Zn^{3-/4-}$). This suggests that formazanate ligands provide a general and tunable redox-active ligand platform, in which the potential at which redox events occur can be rationally modified by substituent effects. Thus, metal complexes with formazanate ligands could show unique properties in (redox) catalysis, an avenue that is currently under investigation in our laboratory.

EXPERIMENTAL SECTION

General Considerations. All manipulations were carried out under a N_2 atmosphere using standard glovebox, Schlenk, and vacuum-line techniques. Toluene, hexane, and pentane (Aldrich, anhydrous, 99.8%) were passed over columns of Al_2O_3 (Fluka), BASF R3-11-supported copper−oxygen scavenger, and molecular sieves (Aldrich, 4 Å). Diethyl ether and THF (Aldrich, anhydrous, 99.8%) were dried by percolation over columns of Al_2O_3 (Fluka). Deuterated solvents were vacuum-transferred from a sodium/potassium alloy (C_6D_6, toluene-d_8, Aldrich) and stored under nitrogen.

Dimethylzinc (Aldrich, 1.2 M in toluene), pentafluorophenylhydrazine (Aldrich, 97%), NaOH (Acros), 2,4,6-trimethylaniline (Aldrich, 98%), aniline (Sigma-Aldrich, 99%), tetrabutylammonium bromide (Sigma-Aldrich, 99%), cyanoacetic acid (Aldrich, 99%), sodium nitrite (Sigma-Aldrich, 99%), sodium carbonate (Merck), phenylhydrazine (Aldrich, 97%), *p*-tolualdehyde (Aldrich, 97%), and *tert*-butyl nitrite (Aldrich, 90%) were used as received. The compounds MesNNC(CN)NNHMes (L8H),[29] $[MesN_2]^+[BF_4]^-$,[19] $MesNHNH_2$·HCl,[30] $[L1]_2Zn$ (**1**),[15] $[L2]_2Zn$ (**2**),[15] and $[L7]_2Zn$ (**7**)[16] were synthesized according to published procedures. The synthesis of the formazan ligands is reported in the SI. NMR spectra were recorded on Varian Gemini 200, VXR 300, Mercury 400, or Varian 500 spectrometers. The ^1H and ^{13}C NMR spectra were referenced internally using the residual solvent resonances and reported in parts per million relative to tetramethylsilane (0 ppm); *J* is reported in hertz. The assignment of NMR resonances was aided by gradient-selected COSY, NOESY, HSQC, and/or HMBC experiments using standard pulse sequences. All electrochemical measurements were performed under an inert N_2 atmosphere in a glovebox using an Autolab PGSTAT 100 computer-controlled potentiostat. CV was performed using a three-electrode configuration comprised of a platinum wire counter electrode, a silver wire pseudoreference electrode, and a platinum disk working electrode (CHI102, CH Instruments; diameter = 2 mm). The platinum working electrode was polished before the experiment using an alumina slurry (0.05 μm), rinsed with distilled water, and subjected to brief ultrasonication to remove any adhered alumina microparticles. The electrodes were then dried in an oven at 75 °C overnight to remove any residual traces of water. The CV data were calibrated by adding ferrocene in a THF solution at the end of the experiments. In all cases, there is no indication that the addition of ferrocene influences the electrochemical behavior of the products. All electrochemical measurements were performed at ambient temperatures under an inert N_2 atmosphere in THF containing 0.1 M

dx.doi.org/10.1021/ic5025873 | *Inorg. Chem.* 2015, 54, 379−388

$[nBu_4N][PF_6]$ as the supporting electrolyte. Data were recorded with *Autolab NOVA* software (version 1.8). UV−vis spectra were recorded in a THF solution (~10^{-5} M) using a Avantes AvaSpec 3648 spectrometer and an AvaLight-DHS light source inside a N_2 atmosphere glovebox. Elemental analyses were performed at the Microanalytical Department of the University of Groningen or Kolbe Microanalytical Laboratory (Mülheim an der Ruhr, Germany).

[MesNNC(*p*-tolyl)NNPh]$_2$Zn ([L3]$_2$Zn, 3). A 1.2 M solution of $ZnMe_2$ in toluene (1.0 mL, 1.2 mmol) was added slowly to a solution of L3H (855.5 mg, 2.4 mmol) in toluene (20 mL) at room temperature. The mixture was stirred for 5 h, after which the volatiles were removed in vacuo. The residue was subsequently extracted into hot hexane (15 mL). Slow cooling of the clear dark-purple solution to −30 °C for 2 days afforded 609 mg of dark crystals of **3** (0.78 mmol, 65%). ^{1}H NMR (400 MHz, C_6D_6, 25 °C): δ 8.25 (d, 2H, J = 8.4 Hz, *p*-tolyl CH), 7.70 (dd, 2H, J = 8.4 and 1.2 Hz, Ph *o*-H), 7.20 (d, 2H, J = 8.0 Hz, *p*-tolyl CH), 6.92 (t, 2H, J = 8.0 Hz, Ph *m*-H), 6.76 (t, 1H, J = 7.4 Hz, Ph *p*-H), 6.38 (s, 2H, Mes CH), 2.20 (s, 3H, *p*-tolyl CH_3), 1.97 (s, 3H, Mes *p*-CH_3), 1.88 (bs, 6H, Mes *o*-CH_3). ^{13}C NMR (100 MHz, C_6D_6, 25 °C): δ 152.9 (Ph *ipso*-C), 148.7 (Mes *ipso*-C), 144.4 (NCN), 137.4 (*p*-tolyl *ipso*-C), 137.1 (*p*-tolyl *C*Me), 130.0 (Ph *m*-CH), 129.8 (*p*-tolyl CH), 128.0 (Ph *p*-CH), 126.5 (*p*-tolyl CH), 121.5 (Ph *o*-CH), 21.6 (*p*-tolyl CH_3). Anal. Calcd for $C_{46}H_{46}N_8Zn$: C, 71.17; H, 5.97; N, 14.43. Found: C, 71.16; H, 6.06; N, 13.82.

[MesNNC(*p*-tolyl)NNMes]$_2$Zn ([L4]$_2$Zn, 4). A 1.2 M solution of $ZnMe_2$ (101.9 μL, 0.122 mmol) in toluene was added to an orange solution containing L4H (97.5 mg, 0.245 mmol) in toluene. The mixture was stirred overnight at 80 °C, after which the solvent was removed in vacuo to give 57.3 mg of compound **4** as a sticky powder (0.067 mmol, 54% yield). Recrystallization by the slow diffusion of pentane into a toluene solution afforded orange crystalline material (16.9 mg, 0.020 mmol, 16% yield). ^{1}H NMR (C_6D_6, 25 °C, 500 MHz): δ 8.04 (d, 4H, J = 7.8 Hz, *p*-tol *o*-H), 7.08 (d, 4H, J = 7.8 Hz, *p*-tol *m*-H), 6.59 (s, 8H, Mes *m*-H), 2.11 (s, 6H, *p*-tol CH_3), 2.08 (s, 12H, Mes *p*-CH_3), 1.88 (s, 24H, Mes *o*-CH_3). ^{13}C NMR (C_6D_6, 25 °C, 126 MHz): δ 149.08 (Mes *ipso*-C), 145.31 (NCN), 137.28 (*p*-tol *p*-C), 136.69 (Mes *p*-C), 136.66 (*p*-tol *ipso*-C), 132.64 (Mes *o*-C), 130.20 (Mes *m*-CH), 129.85 (*p*-tol *m*-CH), 125.65 (*p*-tol *o*-CH), 21.48 (*p*-tol CH_3), 21.15 (Mes *p*-CH_3), 18.29 (Mes *o*-CH_3). Anal. Calcd for $C_{52}H_{58}N_8Zn$: C, 72.58; H, 6.79; N, 13.02. Found: C, 73.13; H, 6.87; N, 13.17.

[C_6F_5NNC(*p*-tolyl)NNPh]$_2$Zn ([L5]$_2$Zn, 5). A 1.2 M solution of $ZnMe_2$ in toluene (0.29 mL, 0.35 mmol) was added slowly to a solution of L5H (273.8 mg, 0.68 mmol) in toluene (15 mL) at room temperature. The mixture was stirred overnight, after which the volatiles were removed in vacuo to afford 237.2 mg of dark crystals of **5** (0.27 mmol, 80%). The product thus obtained was ca. 95% pure. Further purification by recrystallization was not successful. ^{1}H NMR (400 MHz, C_6D_6, 25 °C): δ 8.22 (d, 2H, J = 8.4 Hz, *p*-tolyl CH), 7.50 (d, 2H, J = 7.6 Hz, Ph *o*-CH), 7.19 (d, 2H, J = 8.0 Hz, *p*-tolyl CH), 6.75 (t, 2H, J = 7.6 Hz, Ph *m*-CH), 6.67 (t, 1H, J = 7.6 Hz, Ph *p*-CH), 2.16 (s, 3H, *p*-tolyl CH_3). ^{19}F NMR (375 MHz, C_6D_6, 25 °C): δ −154.4 (dd, 2F, J = 22.5, 5.6 Hz, C_6F_5 *o*-CF), −158.3 (t, 1F, J = 21.5 Hz, C_6F_5 *p*-CF), −162.4 (td, 2F, J = 22.1, 5.2 Hz, C_6F_5 *m*-CF). ^{13}C NMR (100 MHz, C_6D_6, 25 °C): δ 151.7 (Ph *ipso*-C), 145.7 (NCN), 141.1 (dm, J = 255 Hz, C_6F_5), 138.6 (dm, J = 256 Hz, C_6F_5), 137.8 (*p*-tolyl *ipso*-C), 137.7 6 (dm, J = 255 Hz, C_6F_5), 135.6 (*p*-tolyl *p*-C), 129.6 (Ph *m*-C), 129.5 (Ph *p*-C), 129.4 (*p*-tolyl CH), 125.8 (*p*-tolyl CH), 120.5 (Ph *o*-C), 120.4 (C_6F_5 *ipso*-C), 20.8 (*p*-tolyl CH_3).

[C_6F_5NNC(*p*-tolyl)NNMes]$_2$Zn ([L6]$_2$Zn, 6). A 1.2 M solution of $ZnMe_2$ in toluene (0.5 mL, 0.6 mmol) was added slowly to a suspension of L6H (536 mg, 1.2 mmol) in toluene (20 mL) at room temperature. The mixture was stirred overnight, after which the color had changed to intense purple. The volatiles were removed in vacuo, and the residue was subsequently extracted into a hot 3:1 hexane/toluene mixture. Slow cooling of the clear dark-purple solution to −30 °C for 2 days afforded 407 mg of dark-violet crystals of **6** (0.43 mmol, 71%). NMR analysis shows the presence of two predominant isomers in solution; an additional isomer (<5%) was observed in the ^{19}F NMR spectrum, but resonances due to this species could not be separately observed in the ^{1}H NMR spectrum. The ^{13}C NMR spectrum (see the SI) is too complicated to do a full assignment of both isomers separately.

*Major Isomer (**6a**).* ^{1}H NMR (C_6D_6, 400 MHz, 25 °C): δ 8.09 (d, 2H, J = 8.0 Hz, *p*-tolyl CH), 7.22−7.09 (overlapped m, 2H, *p*-tolyl CH), 6.42 (s, 2H, Mes CH), 2.14 (s, 3H, *p*-tolyl *p*-CH_3), 1.98 (s, 9H, Mes *o*-CH_3, *p*-CH_3). ^{19}F NMR (375 MHz, C_6D_6, 25 °C): δ −152.7 (d, 2F, J = 18.0 Hz, C_6F_5 *o*-CF), −160.7 (t, 1F, J = 21.9 Hz, C_6F_5 *p*-CF), −163.3 (td, 2F, J = 21.9 and 4.1 Hz, C_6F_5 *m*-CF).

*Minor Isomer (**6b**).* ^{1}H NMR (C_6D_6, 25 °C): δ 8.25 (d, 2H, J = 8.0 Hz, *p*-tolyl CH), 7.87 (d, 2H, J = 8.0 Hz, *p*-tolyl CH), 7.22−7.09 (overlapped m, 4H, 2 × *p*-tolyl CH), 6.37 (bs, 2H, Mes CH), 6.31 (bs, 2H, Mes CH), 2.20 (s, 3H, *p*-tolyl *p*-CH_3), 2.14 (s, 3H, *p*-tolyl *p*-CH_3), 1.98 (s, 6H, Mes *o*-CH_3), 1.94 (s, 3H, Mes *p*-CH_3), 1.89 (s, 3H, Mes *p*-CH_3), 1.87 (s, 6H, Mes *o*-CH_3). ^{19}F NMR (375 MHz, C_6D_6, 25 °C): δ −153.0 (d, 2F, J = 19.3 Hz, C_6F_5 *o*-CF), −156.3 (d, 2F, J = 21.9 Hz, C_6F_5 *o*-CF), −160.7 (t, 1F, J = 21.9 Hz, C_6F_5 *p*-CF), −162.8 (td, 2F, J = 22.0, 4.7 Hz, C_6F_5 *m*-CF), −165.3 (td, 2F, J = 21.6 and 4.1 Hz, C_6F_5 *m*-CF), −167.6 (t, 1F, J = 21.7 Hz, C_6F_5 *p*-CF).

*Trace Isomer (**6c**).* ^{19}F NMR (375 MHz, C_6D_6, 25 °C): δ −155.2 (bs, 2F, C_6F_5 *o*-CF), −164.2 (t, 2F, J = 20.3 Hz, C_6F_5 *m*-CF), −167.3 (t, 1F, J = 23.5 Hz, C_6F_5 *p*-CF). ^{13}C NMR (100 MHz, C_6D_6, 25 °C): δ 152.3, 149.7 (*p*-tolyl *ipso*-C, **6b**), 148.1 (Mes *ipso*-C, **6a**), 147.8, 146.5 (*p*-tolyl *ipso*-C, **6b**), 146.0 (*p*-tolyl *ipso*-C, **6a**), 141.9 (dm, J = 250.4 Hz, C_6F_5), 141.4 (dm, J = 250.7 Hz, C_6F_5), 139.0 (*p*-tolyl *p*-C, **6b**), 138.9, 138.7 (*p*-tolyl *p*-C, **6b**), 138.7, 138.6 (dm, J = 249.3 Hz, C_6F_5), 138.5 (*p*-tolyl *p*-C, **6a**), 135.6, 135.1, 131.9, 131.5, 131.5, 130.5 (Mes *m*-C, **6a**), 130.1 (Mes *m*-C, **6b**), 129.8, 129.7, 129.5, 128.9 (*p*-tolyl CH, **6b**), 128.5, 128.3, 126.4 (*p*-tolyl CH, **6b**), 126.1 (*p*-tolyl CH, **6a**), 126.0, 21.6, 21.6 (*p*-tolyl *p*-CH_3, **6b**), 21.5 (Mes *p*-CH_3, **6b**), 21.3, 21.0, 20.9, 20.7 (Mes *p*-CH_3, **6b**), 18.3, 17.9 (Mes *o*-CH_3, **6b**). Anal. Calcd for $C_{46}H_{36}F_{10}N_8Zn$: C, 57.78; H, 3.79; N, 11.72. Found: C, 58.66; H, 4.00; N, 11.13.

[PhNNC(*p*-tolyl)NNPh][MesNNC(CN)NNMes]Zn ([L1][L8]Zn, 8). A flask was charged with [PhNNC(*p*-tol)NNPh]ZnMe (783 mg, 2.0 mmol), L8H (663 mg, 2.0 mmol), and toluene (20 mL). The reaction mixture was stirred at room temperature for 2 h, after which the volatiles were removed in vacuo, and the residue was subsequently extracted into a hot 1:1 hexane/toluene mixture. Slow cooling of the clear dark-purple solution to −30 °C for 2 days afforded 796 mg of dark-violet crystals of **8** (1.12 mmol, 56%). NMR analysis shows the presence of two isomers in solution. The ^{13}C NMR spectrum (see the SI) is too complicated to do a full assignment of both isomers separately.

*Major Isomer (**8a**).* ^{1}H NMR (400 MHz, C_6D_6, 25 °C): δ 7.98 (d, 2H, J = 8.4 Hz, p-tolyl CH), 7.51 (d, 4H, J = 8.4 Hz, Ph *o*-H), 7.21 (d, 2H, J = 8.0 Hz, *p*-tolyl CH), 6.95 (t, 4H, J = 8.0 Hz, Ph *m*-H), 6.85 (t, 2H, J = 7.6 Hz, Ph *p*-H), 6.55 (s, 2H, Mes *m*-CH), 6.32 (s, 2H, Mes *m*-CH), 2.24 (s, 3H, Mes *p*-CH_3), 2.21 (s, 6H, Mes *o*-CH_3), 1.94 (s, 3H, *p*-tolyl CH_3), 1.59 (s, 3H, Mes *p*-CH_3), 1.56 (s, 6H, Mes *o*-CH_3).

*Minor Isomer (**8b**).* ^{1}H NMR (400 MHz, C_6D_6, 25 °C): δ 8.14 (d, 2H, J = 8.4 Hz, *p*-tolyl CH), 7.33 (d, 4H, J = 7.6 Hz, Ph *o*-CH), 7.19−7.13 (m, 2H, *p*-tolyl CH), 6.98−6.92 (m, 4H, Ph *m*-CH), 6.80 (t, 2H, J = 7.4 Hz, Ph *p*-H), 2.18 (s, 3H, Mes *p*-CH_3), 1.94 (s, 3H, *p*-tolyl CH_3), 1.84 (s, 6H, Mes *o*-CH_3). ^{13}C NMR (100 MHz, C_6D_6, 25 °C): δ 152.4 (Ph *ipso*-C, **8b**), 151.9 (Ph *ipso*-C, **8a**), 150.9 (Mes *ipso*-C, **8a**), 146.4 (Mes *ipso*-C, **8b**), 145.5 (Mes *ipso*-C, **8a**), 143.3, 142.4 (*p*-tolyl *ipso*-C, **8a**), 138.3 (Mes *p*-C, **8a**), 137.6 (Mes *ipso*-C, **8b**), 136.8, 136.6 (Mes *p*-C, **8a**), 136.0 (*p*-tolyl *p*-C, **8a**), 131.4, 130.9 (Mes *p*-C, **8a**), 130.6 (Mes *m*-CH, **8a**), 130.0 (Mes *m*-CH, **8b**), 129.8 (Mes *m*-CH, **8a**), 129.4 (Ph *m*-H, **8a**), 129.3, 129.0 (*p*-tolyl CH, **8b**), 128.8, 128.2 (Ph *p*-H, **8b**), 127.8, 127.5, 126.4, 125.8 (*p*-tolyl CH, **8a**), 125.8 (*p*-tolyl CH, **8b**), 125.5, 120.0 (*p*-tolyl CH, **8b**), 119.6 (Ph *o*-H, **8a**), 117.9, 113.0, 20.8 (Mes *p*-CH_3, **8a**), 20.3, 20.3 (Mes *o*-CH_3, **8b**), 20.1 (Mes *p*-CH_3, **8a**), 19.5 (Mes *o*-CH_3, **8a**), 18.0 (Mes *o*-CH_3, **8b**), 17.0 (Mes *o*-CH_3, **8a**). Anal. Calcd for $C_{40}H_{39}N_9Zn$: C, 67.55; H, 5.53; N, 17.73. Found: C, 67.79; H, 5.58; N, 17.24.

[PhNNC(*p*-tolyl)NNHPh]Zn(C_6F_5)$_2$ ([L1H]Zn(C_6F_5)$_2$, 9). Toluene (3 mL) was added onto a mixture of Zn(C_6F_5)$_2$ (100 mg, 0.25 mmol) and PhNNC(ptol)NNHPh (78.7 mg, 0.25 mmol). An immediate

dx.doi.org/10.1021/ic5025873 | *Inorg. Chem.* 2015, 54, 379−388

Table 4. Crystallographic Data for 3, 4, 6, 8, and 9

	3	4	6	8	9
chemical formula	$C_{46}H_{46}N_8Zn$	$C_{52}H_{58}N_8Zn$	$C_{46}H_{36}F_{10}N_8Zn$	$C_{40}H_{39}N_9Zn$	$C_{32}H_{18}F_{10}N_4Zn{\cdot}0.5C_7H_8$
M_r	776.28	860.43	956.20	711.17	759.94
cryst syst	monoclinic	triclinic	monoclinic	monoclinic	triclinic
color, habit	violet, block	dark red, needle	purple, block	violet, block	red, block
size (mm)	0.28 × 0.40 × 0.46	0.08 × 0.09 × 0.21	0.23 × 0.52 × 0.80	0.19 × 0.16 × 0.09	0.30 × 0.38 × 0.63
space group	$C2/c$ (No. 15)	$P\bar{1}$ (No. 2)	$P2_1/n$ (No. 14)	$P2_1/c$ (No. 14)	$P1$ (No. 1)
a (Å)	17.9988(6)	11.1353(6)	11.1564(4)	15.070(4)	10.8546(3)
b (Å)	11.4774(5)	12.0886(7)	16.0507(5)	12.864(3)	10.9884(3)
c (Å)	19.3454(5)	17.9233(9)	24.0955(10)	19.235(5)	13.7821(4)
α (deg)		75.379(2)			82.9604(7)
β (deg)	96.906(1)	87.426(2)	101.165(3)	104.010(8)	85.6641(8)
γ (deg)		76.677(2)			78.0685(7)
V (Å^3)		2271.5(2)	4233.1(3)	3618.2(15)	1594.08(8)
Z	4	2	4	4	2
ρ_{calc} (g·cm^{-3})	1.300	1.258	1.500	1.306	1.583
radiation, λ (Å)	Mo Kα, 0.71073	Mo Kα, 0.71073	Mo Kα, 0.71073	Mo Kα, 0.71073	Cu Kα, 1.54184
μ(Mo Kα) (mm^{-1})	0.663	0.586	0.669	0.721	
μ(Cu Kα) (mm^{-1})					1.903
F(000)	1632	912	1952	1488	766
temp (K)	150(2)	100(2)	150(2)	100(2)	100(2)
θ range (deg)	2.1−27.5	2.75−27.13	1.5−27.5	2.1−27.9	3.2−56.7
data collected (h, k, l)	−23:22, −14:14, −25:23	−14:14, −15:15, −22:21	−14:14, −20:20, −30:31	−19:19, −16:16, −25:25	−11:9, −11:11, −14:11
no. of reflns collected	28246	75805	48788	99698	14215
no. of indep reflns	4542	10034	9672	8651	5237
obsd reflns $F_o \geq 2.0\sigma(F_o)$	4357	8037	7477	7215	5236
$R(F)$ [obsd reflns] (%)	2.54	4.04	5.08	3.39	2.78
$R_w(F^2)$ [all reflns] (%)	7.33	9.41	14.28	8.69	7.43
GOF	1.04	1.043	1.04	1.04	1.03
weighting a, b	0.0391, 3.9002	0.0368, 1.7988	0.0677, 4.5821	0.0375 2.0127	0.0513, 0.8707
params refined	253	564	594	458	914
Flack x parameter[36]					0.49(2)
min, max residual densities	−0.41, 0.39	−0.39, 0.42	−0.52, 0.88	−0.38, 0.36	−0.27, 0.40

reaction was observed, and after stirring for ca. 15 min, all volatiles were removed in vacuo. The residue was suspended in hexane (ca. 5 mL), and toluene was added dropwise until a clear solution was obtained. Cooling to −80 °C overnight precipitated a crystalline material, from which the supernatant was decanted. Drying under vacuum resulted in 108 mg of **9**·0.5toluene as red blocks (0.14 mmol, 57%). ^{1}H NMR (400 MHz, C_6D_6, 25 °C): δ 8.20 (s, 1H, NH), 7.98 (d, 2H, J = 7.5 Hz, N═NPh *o*-H), 7.33 (d, 2H, J = 7.7 Hz, *p*-tolyl *o*-H), 7.00 (d, 2H, J = 7.7 Hz, *p*-tolyl *m*-H), 6.88 (t, 1H, overlapped, N═NPh *p*-H), 6.86 (t, 2H, overlapped, N═NPh *m*-H), 6.84 (t, 2H, overlapped, NNHPh *m*-H), 6.71 (d, 2H, J = 7.7 Hz, NNHPh *o*-H), 6.66 (t, 1H, J = 7.4 Hz, NNHPh *p*-H), 2.05 (s, 3H, *p*-tolyl CH_3). ^{13}C NMR (100.6 MHz, C_6D_6, 25 °C): δ 151.2 (NCN), 149.8 (s, N═NPh *ipso*-C), 142.4 (s, *p*-tolyl CMe), 140.1 (s, NNHPh *ipso*-C), 134.0 (d, J = 163 Hz, N═NPh *p*-CH), 131.0 (d, J = 160, *p*-tolyl *m*-CH), 130.1 (d, J = 163 Hz, N═NPh *m*-CH), 129.9 (d, J = 162 Hz, NNHPh *m*-CH), 128.9 (d, J = 161 Hz, *p*-tolyl *o*-CH), 126.4 (d, J = 164 Hz, NNHPh *p*-CH), 126.3 (s, *p*-tolyl *ipso*-C), 123.8 (d, J = 163 Hz, N═NPh *o*-CH), 118.0 (d, J = 161 Hz, NNHPh *o*-CH), 21.3 (q, J = 126.9 Hz, *p*-tolyl CH_3). ^{19}F NMR (376.3 MHz, C_6D_6, 25 °C): δ −118.2 (d, 2F, J = 26.6 Hz, *o*-F), −156.5 (t, 1F, J = 18.1 Hz, *p*-F), −161.9 (m, 2F, *m*-F). Anal. Calcd for $C_{35.5}H_{22}F_{10}N_4Zn$: C, 56.11; H, 2.92; N, 7.37. Found: C, 55.95; H, 2.89; N, 7.47.

X-ray Crystal Structures. Suitable crystals of **3**, **4**, **6**, **8**, and **9** were mounted and transferred into the cold nitrogen stream of a Bruker D8 Venture (for **4** and **8**), a Bruker Kappa Apex II diffractometer (for **3** and **6**; both sealed tube, λ = 0.71073 Å), or a Bruker Proteum diffractometer (for compound **9**; rotating anode, λ = 1.54184 Å). Integration of the X-ray intensities was performed with *Eval15*[31] for compounds **3** and **6** and with *SAINT*[32] for compounds **4**, **8**, and **9**. Intensity data were corrected for Lorentz and polarization effects, scale variation, and decay and absorption: a multiscan absorption correction was applied, based on the intensities of symmetry-related reflections measured at different angular settings (*SADABS*).[32,33] The structures were solved with *SHELXS*[34] (**3**, **4**, **6**, and **8**) or *SHELXT*[35] (**9**). The H atoms were located in the difference Fourier maps (**3** and **6**) or generated by geometrical considerations, constrained to idealized geometries, and allowed to ride on their carrier atoms with an isotropic displacement parameter related to the equivalent displacement parameter of their carrier atoms (**4** and **8**). Structure refinement was performed with the program package *SHELXL*.[34] For compound **9**, two data sets were measured on the same crystal. At 200(2) K, the space group is centrosymmetric $P\bar{1}$ (No. 2). The toluene molecule is disordered on an inversion center (occupancy $^1/_2$), and one of the C_6F_5 moieties is disordered as well. Restraints were used to model the disorder. After cooling to 100(2) K and a solid−solid phase transition, the structure becomes an inversion twin in the noncentrosymmetric

dx.doi.org/10.1021/ic5025873 | *Inorg. Chem.* 2015, 54, 379−388

space group *P*1 (No. 1). The structure is well ordered in this low-temperature phase. Crystal data and details on data collection and refinement are presented in Table 4.

■ ASSOCIATED CONTENT

Ⓢ Supporting Information

Synthesis and characterization data for all new ligands, cyclic voltammograms for compounds **1**−**8**, NMR spectra for compounds **6** and **8**, and CIF files for **3**, **4**, **6**, **8**, and **9**. This material is available free of charge via the Internet at http://pubs.acs.org.

■ AUTHOR INFORMATION

Corresponding Author

*E-mail: edwin.otten@rug.nl.

Author Contributions

The manuscript was written through contributions of all authors. All authors have given approval to the final version of the manuscript.

Notes

The authors declare no competing financial interest.

■ ACKNOWLEDGMENTS

E.O. thanks The Netherlands Organisation for Scientific Research (NWO) for financial support (Veni grant). The Apex and Proteum diffractometers (Utrecht University) were financed by NWO.

■ REFERENCES

(1) (a) Ernst, R. D. *Comments Inorg. Chem.* **1999**, *21*, 285. (b) Rajapakshe, A.; Gruhn, N. E.; Lichtenberger, D. L.; Basta, R.; Arif, A. M.; Ernst, R. D. *J. Am. Chem. Soc.* **2004**, *126*, 14105. (c) Paz-Sandoval, M. A.; Rangel-Salas, I. I. *Coord. Chem. Rev.* **2006**, *250*, 1071. (d) Stahl, L.; Ernst, R. D. In *Advances in Organometallic Chemistry*; West, R., Hill, A. F., Fink, M. J., Eds.; Academic Press: New York, 2007; Vol. *55*, p 137.

(2) Bourget-Merle, L.; Lappert, M. F.; Severn, J. R. *Chem. Rev.* **2002**, *102*, 3031.

(3) (a) Siedle, A. R.; Webb, R. J.; Behr, F. E.; Newmark, R. A.; Weil, D. A.; Erickson, K.; Naujok, R.; Brostrom, M.; Mueller, M.; Chou, S.-H.; Young, V. G. *Inorg. Chem.* **2003**, *42*, 932. (b) Siedle, A. R.; Webb, R. J.; Brostrom, M.; Newmark, R. A.; Behr, F. E.; Young, V. G. *Organometallics* **2004**, *23*, 2281.

(4) (a) Dias, H. V. R.; Singh, S. *Inorg. Chem.* **2004**, *43*, 5786. (b) Dias, H. V. R.; Singh, S. *Inorg. Chem.* **2004**, *43*, 7396. (c) Flores, J. A.; Badarinarayana, V.; Singh, S.; Lovely, C. J.; Dias, H. V. R. *Dalton Trans.* **2009**, 7648. (d) Dias, H. V. R.; Flores, J. A.; Wu, J.; Kroll, P. *J. Am. Chem. Soc.* **2009**, *131*, 11249. (e) Adiraju, V. A. K.; Flores, J. A.; Yousufuddin, M.; Dias, H. V. R. *Organometallics* **2012**, *31*, 7926.

(5) Walther, M.; Wermann, K.; Lutsche, M.; Günther, W.; Görls, H.; Anders, E. *J. Org. Chem.* **2006**, *71*, 1399.

(6) Zhou, M.; Gong, T.; Qiao, X.; Tong, H.; Guo, J.; Liu, D. *Inorg. Chem.* **2011**, *50*, 1926.

(7) (a) Häger, I.; Fröhlich, R.; Würthwein, E.-U. *Eur. J. Inorg. Chem.* **2009**, *2009*, 2415. (b) Heße, N.; Fröhlich, R.; Humelnicu, I.; Würthwein, E.-U. *Eur. J. Inorg. Chem.* **2005**, *2005*, 2189.

(8) (a) Kopylovich, M. N.; Kirillov, A. M.; Tronova, E. A.; Haukka, M.; Kukushkin, V. Y.; Pombeiro, A. J. L. *Eur. J. Inorg. Chem.* **2010**, *2010*, 2425. (b) Kopylovich, M. N.; Lasri, J.; Guedes da Silva, M. F. C.; Pombeiro, A. J. L. *Dalton Trans.* **2009**, 3074. (c) Kopylovich, M. N.; Pombeiro, A. J. L. *Coord. Chem. Rev.* **2011**, *255*, 339.

(9) Nineham, A. W. *Chem. Rev.* **1955**, *55*, 355.

(10) Grychtol, K.; Mennicke, W. In *Ullmann's Encyclopedia of Industrial Chemistry*; Wiley-VCH Verlag GmbH & Co. KGaA: Weinheim, Germany, 2000.

(11) (a) Rush, R. M.; Yoe, J. H. *Anal. Chem.* **1954**, *26*, 1345. (b) Säbel, C. E.; Neureuther, J. M.; Siemann, S. *Anal. Biochem.* **2010**, *397*, 218.

(12) Seidler, E. *Prog. Histochem. Cytochem.* **1991**, *24*, 1.

(13) (a) Gilroy, J. B.; Ferguson, M. J.; McDonald, R.; Hicks, R. G. *Inorg. Chim. Acta* **2008**, *361*, 3388. (b) Gilroy, J. B.; Patrick, B. O.; McDonald, R.; Hicks, R. G. *Inorg. Chem.* **2008**, *47*, 1287. (c) Hong, S.; Hill, L. M. R.; Gupta, A. K.; Naab, B. D.; Gilroy, J. B.; Hicks, R. G.; Cramer, C. J.; Tolman, W. B. *Inorg. Chem.* **2009**, *48*, 4514.

(14) Gilroy, J. B.; Ferguson, M. J.; McDonald, R.; Patrick, B. O.; Hicks, R. G. *Chem. Commun.* **2007**, 126.

(15) Chang, M.-C.; Dann, T.; Day, D. P.; Lutz, M.; Wildgoose, G. G.; Otten, E. *Angew. Chem., Int. Ed.* **2014**, *53*, 4118.

(16) Chang, M. C.; Otten, E. *Chem. Commun.* **2014**, *50*, 7431.

(17) (a) Barbon, S. M.; Reinkeluers, P. A.; Price, J. T.; Staroverov, V. N.; Gilroy, J. B. *Chem.—Eur. J.* **2014**, *20*, 11340. (b) Barbon, S. M.; Price, J. T.; Reinkeluers, P. A.; Gilroy, J. B. *Inorg. Chem.* **2014**, *53*, 10585−10593.

(18) Neugebauer, F. A.; Trischmann, H. *Justus Liebigs Ann. Chem.* **1967**, *706*, 107.

(19) Doyle, M. P.; Bryker, W. J. *J. Org. Chem.* **1979**, *44*, 1572.

(20) (a) Zhu, D.; Budzelaar, P. H. M. *Dalton Trans.* **2013**, *42*, 11343. (b) We thank Prof. Peter Budzelaar and Arjan Koekoek (University of Manitoba) for sharing the synthesis procedure to make L4H..

(21) (a) Cheng, M.; Moore, D. R.; Reczek, J. J.; Chamberlain, B. M.; Lobkovsky, E. B.; Coates, G. W. *J. Am. Chem. Soc.* **2001**, *123*, 8738. (b) Peng, Y.-L.; Hsueh, M.-L.; Lin, C.-C. *Acta Crystallogr., Sect. E* **2007**, *63*, m2388. (c) Schulz, S.; Eisenmann, T.; Bläser, D.; Boese, R. *Z. Anorg. Allg. Chem.* **2009**, *635*, 995. (d) Vaughan, B. A.; Wetherby, A. E.; Waterman, R. *Acta Crystallogr., Sect. E* **2012**, *68*, m343.

(22) (a) Martinez, C. R.; Iverson, B. L. *Chem. Sci.* **2012**, *3*, 2191. (b) Salonen, L. M.; Ellermann, M.; Diederich, F. *Angew. Chem., Int. Ed.* **2011**, *50*, 4808.

(23) (a) Balt, S.; Renkema, W. E. *Inorg. Chim. Acta* **1977**, *22*, 161. (b) Balt, S.; Meuldijk, J.; Renkema, W. E. *Inorg. Chim. Acta* **1980**, *43*, 173.

(24) Meuldijk, J.; Renkema, W. E.; van Herk, A. M.; Stam, C. H. *Acta Crystallogr., Sect. C* **1983**, *39*, 1536.

(25) Travieso-Puente, R.; Chang, M.-C.; Otten, E. *Dalton Trans.* **2014**, *43*, 18035.

(26) Full details on the synthesis of mono(formazanate)zinc complexes will be published in due course.

(27) (a) Mountford, A. J.; Lancaster, S. J.; Coles, S. J.; Horton, P. N.; Hughes, D. L.; Hursthouse, M. B.; Light, M. E. *Organometallics* **2006**, *25*, 3837. (b) Martin, E.; Spendley, C.; Mountford, A. J.; Coles, S. J.; Horton, P. N.; Hughes, D. L.; Hursthouse, M. B.; Lancaster, S. J. *Organometallics* **2008**, *27*, 1436. (c) Neu, R. C.; Otten, E.; Stephan, D. W. *Angew. Chem., Int. Ed.* **2009**, *48*, 9709. (d) Schnee, G.; Fliedel, C.; Avilés, T.; Dagorne, S. *Eur. J. Inorg. Chem.* **2013**, *2013*, 3699. (e) Tskhovrebov, A. G.; Vuichoud, B.; Solari, E.; Scopelliti, R.; Severin, K. *J. Am. Chem. Soc.* **2013**, *135*, 9486.

(28) (a) Gilroy, J. B.; McKinnon, S. D. J.; Kennepohl, P.; Zsombor, M. S.; Ferguson, M. J.; Thompson, L. K.; Hicks, R. G. *J. Org. Chem.* **2007**, *72*, 8062. (b) Hicks, R. G.; Öhrström, L.; Patenaude, G. W. *Inorg. Chem.* **2001**, *40*, 1865.

(29) Gilroy, J. B.; Otieno, P. O.; Ferguson, M. J.; McDonald, R.; Hicks, R. G. *Inorg. Chem.* **2008**, *47*, 1279.

(30) Carlin, R. B.; Moores, M. S. *J. Am. Chem. Soc.* **1962**, *84*, 4107.

(31) Schreurs, A. M. M.; Xian, X.; Kroon-Batenburg, L. M. J. *J. Appl. Crystallogr.* **2010**, *43*, 70.

(32) *APEX2 v2012.4-3*, *SAINT* (version 8.18C), and *SADABS* (version 2012/1); Bruker AXS Inc.: Madison, WI, 2012.

(33) Sheldrick, G. M. *SADABS: Area-Detector Absorption Correction*; Universität Göttingen: Göttingen, Germany, 1999.

(34) Sheldrick, G. *Acta Crystallogr., Sect. A* **2008**, *64*, 112.

(35) Sheldrick, G. M. *SHELXT*; Universität Göttingen: Göttingen, Germany, 2013,

(36) Flack, H. *Acta Crystallogr., Sect. A* **1983**, *39*, 876.